Biochimica et Biophysica Acta 1828 (2013) 1674–1682

Contents lists available at SciVerse ScienceDirect

Biochimica et Biophysica Acta

journal homepage: www.elsevier.com/locate/bbamem

Observing the translocation of a mitochondria-penetrating peptide with solid-state NMR

Lauren E. Marbella *, Hyo Soon Cho, Megan M. Spence

Department of Chemistry, University of Pittsburgh, Chevron Science Center, 219 Parkman Avenue, Pittsburgh, PA 15260, USA

ARTICLE INFO

Article history:
Received 5 January 2013
Received in revised form 25 March 2013
Accepted 29 March 2013
Available online 6 April 2013

Keywords:
Penetrating peptides
Mitochondria targeting
Solid state NMR spectroscopy
Translocation mechanism
Electroporation

ABSTRACT

A new class of penetrating peptides that can target the mitochondria with high specificity was recently discovered. In this work, we developed a model inner mitochondrial membrane, equipped with a transmembrane gradient, suitable for solid-state NMR experiments. Using solid-state NMR, we observed a mitochondria-penetrating peptide interacting with the model inner mitochondrial membrane to gain insight into the mechanism of translocation. The paramagnetic relaxation effect due to Mn^{2+} ions on ^{13}C magic angle spinning NMR was used to measure the insertion depth of the peptide and its distribution in each monolayer of the membrane. We found that at low peptide concentration the peptide binds to the outer leaflet and at high concentration, it crosses the hydrophobic bilayer core and is distributed in both leaflets. In both concentration regimes, the peptide binds at the C2 position on the lipid acyl chain. The mitochondria-penetrating peptide crossed to the inner leaflet of the model membranes without disrupting the lamellarity. These results provide evidence that supports the electroporation model of translocation. We estimated the energy associated with crossing the inner mitochondrial membrane. We found that the transmembrane potential provides sufficient energy for the peptide to cross the hydrophobic core, which is the most unfavorable step in translocation.

1. Introduction

Mitochondria are an interesting target for drug delivery due to their role in energy production, reactive oxygen species production, and apoptosis [1–9]. Drug delivery to the mitochondria is difficult due to the intricacies involved in crossing three diverse membranes (Fig. 1): the plasma membrane, and the outer and inner mitochondrial membranes (OMM and IMM, respectively) [10–13]. Overcoming these challenges, a new class of synthetically designed peptides was recently discovered to penetrate the plasma membrane and target the mitochondria with high specificity, coined mitochondria-penetrating peptides (MPPs) [10]. By targeting the mitochondria directly, MPPs become a valuable vehicle for drug delivery. For instance, methotrexate is a powerful antibacterial agent, but accumulation in the cytosol of human cells renders it highly toxic and limits its therapeutic capabilities [14]. By conjugating methotrexate to MPPs, the drug specifically targeted the mitochondria, decreasing the toxicity three orders of magnitude, while maintaining antibacterial activity [14]. However, the mechanism by which MPPs are able to reach the mitochondrial matrix remains unknown. Due to the resolution limit of confocal microscopy, the outer and inner mitochondrial membranes cannot be resolved with fluorescence techniques and it is impossible to determine whether or not the MPPs remain bound to the inner mitochondrial membrane or cross this barrier to localize in the matrix.

Solid-state nuclear magnetic resonance (ssNMR) is a useful tool to study peptide–lipid interactions with atomic scale resolution. Recent studies have proven that ssNMR is vital to evaluate membrane interaction with antimicrobial peptides [15–22], cell-penetrating peptides [23–25], channel-forming peptides [18,26,27], and viruses [18,28–30]. Several model membrane formulations have been reported to examine the interplay between various peptides and plasma membranes. Recent studies have shown that membrane composition, specifically headgroup functionality, and transmembrane potential play important roles in membrane–peptide activity by controlling peptide binding and subsequent bilayer disruption or alteration [18,19,31–37]. The recent development of MPPs presents the need to develop an accurate model of inner mitochondrial membranes that is well suited for ssNMR measurements. The combination of model inner mitochondrial membranes and ssNMR provides the platform to study the MPP effect on the bilayer lamellarity as well as membrane insertion depth, in order to gain insight into the mechanism of translocation.

In general, penetrating peptides are small, water soluble peptides with many cationic and hydrophobic residues [38–40]. These peptides are able to cross membranes in a highly efficient, non-lytic fashion to deliver cargo to the interior of cells, but the mechanism of translocation remains unknown [38–40]. Several proposed models exist to describe the apparent energy-independent mode of membrane penetration, including the inverse micelle model [41,42], the electroporation model [43,44], and the guanidinum-phosphate complexation model [24], all of which show distinct spectroscopic signatures. By utilizing static ^{31}P and paramagnetic relaxation enhancement (PRE) ssNMR techniques,

* Corresponding author. Tel.: +1 412 648 9917.
E-mail address: lem64@pitt.edu (L.E. Marbella).

0005-2736/$ – see front matter © 2013 Elsevier B.V. All rights reserved.
http://dx.doi.org/10.1016/j.bbamem.2013.03.027

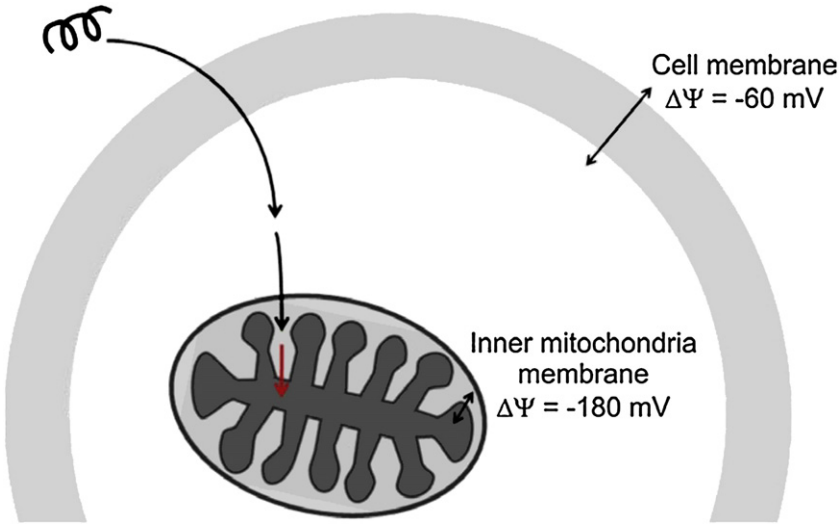

Fig. 1. Membrane barriers encountered by mitochondria-penetrating peptides. Cell penetrating peptides only cross the plasma membrane. Mitochondria-penetrating peptides must cross a total of three membranes; the plasma membrane and the outer and inner mitochondrial membranes to reach the matrix.

we are able to gain information on lamellar integrity, bilayer sidedness, and peptide insertion depth, in order to differentiate between each model.

The peptide–lipid interaction is believed to be a vital step in the translocation. The favorable interaction between cationic peptides and negatively charged phospholipid headgroups is thought to be the first step in translocation, and is shared by penetrating peptides [18,23–25,45], antimicrobial peptides [20,21,31,46–49], and voltage gated channel-forming peptides [26,27,50]. In the inverse micelle model, the peptide remains bound at the membrane–water interface throughout translocation and the formation of inverse micelles permits passage to the membrane interior [41,42]. The presence of an inverse micelle phase produces an isotropic peak in ^{31}P powder pattern which is consistent with a disruption of the native lamellar character and the rapid tumbling of micelles [51–53].

In the electroporation and guanidinium-phosphate complexation models, the cationic peptide charge and anionic lipid charge are believed to play a role in both initial peptide–lipid interaction, as well as the translocation mechanism. In the electroporation model, the negatively charged phospholipid headgroup on the outer leaflet of the bilayer binds the cationic penetrating peptide, until the remaining anionic surface change reaches a critical value [43]. When the peptide concentration exceeds this threshold, the asymmetrically bound peptides on the outer leaflet create an electric field between the differently charged outer and inner monolayers [43]. The transbilayer electric field destabilizes the membrane and the peptide crosses the hydrophobic core in an electroporation-like fashion to bind to the inner leaflet of the bilayer [43]. Therefore, if the peptide is internalized via the electroporation model, we would expect to observe binding only to the outer leaflet at low peptide concentrations, and binding to both the inner and outer leaflets at high peptide concentrations.

The guanidinium-phosphate complexation model proposes that the cationic arginine residues on the peptide bind electrostatically to the anionic phosphate groups present on the lipid headgroups. By neutralizing the highly cationic charge, the peptides are able to cross the bilayer without a high free-energy penalty [24]. Since this mechanism does not require charge accumulation to destabilize the membrane, we expect that at both high and low concentrations, the peptide will bind to both the inner and outer leaflets of the bilayer [24].

To determine the mode of MPP translocation, we used ^{13}C magic angle spinning (MAS) PRE NMR to create a system that can distinguish bilayer sidedness and probe peptide insertion depth, which in turn, will differentiate between the electroporation and guanidinium-phosphate complexation models. To assess bilayer lamellarity during peptide insertion, we used variable temperature static ^{31}P NMR measurements. Both static ^{31}P and ^{2}H NMR measurements are sensitive to alterations in membrane integrity [20,22,53–59]. In the ^{13}C PRE method, paramagnetic ions bind to membranes and cause line broadening and subsequent signal reduction in the NMR spectra by enhancing the T_2 relaxation rate [60,61]. The PRE effect is distance dependent and can distinguish each leaflet of the bilayer so the signal attenuation serves as a spectroscopic ruler for molecular location in the membrane [24,62,63]. The NMR relaxation enhancement due to the addition of paramagnetic ions and tags has been exploited to provide long distance measurements for protein structure determination [28,64–68], rapid acquisition of membrane-bound protein spectra [69,70], probe protein-biomolecule and small molecule interactions [56,71,72], distinguish between inner and outer leaflets of lipid bilayers [24,62,63], manipulate bicelle orientation [73], and measure immersion depth in membrane systems [24,74].

For our ssNMR study, we chose a peptide with high mitochondrial localization with the amino acid sequence Cha–Arg–Cha–Lys, where Cha = cyclohexylalanine. We constructed large unilamellar vesicles (LUVs) with a transmembrane gradient of about −180 mV, composed of a mixture of cardiolipin (CL, 10% mol), phosphatidylcholine (PC, 50% mol), and phosphatidylethanolamine (PE, 40% mol). We chose to incorporate an electrochemical gradient in our model membranes because translocation of the MPPs was shown to be highly dependent on electrochemical potential [10]. We compared the spectra from three different peptide–lipid systems: Mn^{2+} free, Mn^{2+} bound to one side of the vesicle, and Mn^{2+} bound to both the inside and outside of the vesicle. We were able to establish a sustainable model of inner mitochondrial membranes for ssNMR measurements and found that the MPP does not alter the bilayer integrity. At low peptide concentrations, the MPP binds to the outer leaflet only, whereas at high concentrations the MPP is distributed into both leaflets, following the electroporation model for translocation into the mitochondria.

2. Materials and methods

2.1. Materials

All lipid products used to form the model mitochondrial membranes are commercially available, including 1,1′,2,2′-tetraoleoyl cardiolipin sodium salt (18:1 CL), 1-palmitoyl-2-linoleoyl-sn-glycero-3-phosphocholine (16:0–18:2 PC), and 1,2-distearoyl-sn-glycero-3-

phosphoethanolamine (18:0 PE), and were purchased from Avanti Polar Lipids, Inc. (Alabaster, AL). The mitochondria-penetrating peptide (Cha–Arg–Cha–Lys) was purchased from AnaSpec, Inc. (Freemont, CA) with uniformly labeled ^{13}C, ^{15}N residues at positions R2 and K4 at >95% purity. All other chemicals were purchased from Thermo Fisher Scientific (Pittsburgh, PA) and used as received.

2.2. Model mitochondria membrane sample preparation

We constructed large unilamellar vesicles (LUVs) that exhibited a transmembrane gradient according to two known protocols [75,76]. A pH difference was used to establish a transmembrane gradient. The membrane encapsulated 300 mM pH 4 phosphate buffer inside the vesicle and 10 mM pH 7 phosphate buffer outside to establish an electrochemical potential of −177 mV, which is reflective of the biologically encountered mitochondrial gradient of −180 mV. The existence of a three unit pH gradient in our system was confirmed by the fluorescence response of 9-aminoacridine as previously described [77].

Hydrated CL/PC/PE membranes were formed by dissolving the lipids in a 95:5 benzene:ethanol mixture at an appropriate molar ratio of 0.1/0.5/0.4, respectively. The lipid mixture was lyophilized overnight. The dried lipid cake was rehydrated with 300 mM phosphate buffer at pH 4 which was heated to 85 °C. The rehydrated lipid sample was incubated for 2 h at 85 °C and vortexed periodically to produce multilamellar vesicles (MLVs). The resulting MLVs were down-sized using a mini extruder (Avanti Polar Lipids, Inc.) and passed through a 100 nm polycarbonate membrane 21 times to consistently produce LUVs of uniform diameter of 100 nm. The size of the vesicles was confirmed by dynamic light scattering on a ZetaPALS particle size analyzer. The LUVs were dialyzed for at least 8 h using a Slide-A-Lyzer (Thermo Fisher Scientific) to remove the low pH, high salt buffer and replace it with 10 mM phosphate buffer at pH 7 for the exterior membrane environment.

After dialysis, the MPP was added at the appropriate molar ratio (P:L = 1:10 or P:L = 1:40) to the LUVs and incubated overnight. The MPP–lipid mixture was centrifuged at 160,000 *g* for 1.5 h to yield a hydrated pellet, which was packed into a 200 μL MAS rotor. For the Mn^{2+} containing samples, the Mn^{2+} solution was prepared from $MnCl_2 \cdot 4H_2O$ and added at 8 mol% of the lipids. To obtain one side Mn^{2+} bound vesicles, the Mn^{2+} solution was either added after ultracentrifugation or during extrusion, producing outside-bound and inside-bound one side Mn^{2+} bound samples. For two side Mn^{2+} bound vesicles, the vesicles were extruded with the appropriate percentage of Mn^{2+} and had Mn^{2+} added after dialysis to replace the ions lost during this process.

2.3. NMR spectroscopy

All NMR measurements were performed on a Bruker Avance 500 (11.7 T) spectrometer operating at a resonant frequency of 500 MHz for ^{1}H, 202 MHz for ^{31}P, and 125 MHz for ^{13}C, equipped with a BCU05 Variable Temperature Control Unit. Data was processed using Bruker Topspin 1.3 or iNMR software. All experiments were performed using a Bruker HXY broadband MAS probehead doubly tuned to $^{1}H/^{13}C/Y$ or $^{1}H/^{31}P/Y$. ^{13}C chemical shifts were externally referenced to adamantane at 38.5 ppm on the TMS scale. ^{31}P chemical shifts were referenced to 85% phosphoric acid at 0.0 ppm. ^{15}N chemical shifts were referenced to glycine at 109.4 ppm. The spinning rate for all MAS experiments was 5 kHz and each experiment was performed at 310 K, unless otherwise indicated. ^{13}C direct polarization (DP) MAS NMR spectra were decoupled with two pulse phase modulation (TPPM) at ^{1}H field strengths of 30 kHz. Typical radiofrequency (rf) pulse lengths were ~5 μs for ^{13}C and ~2 μs for ^{1}H. Static ^{31}P spectra were decoupled with WALTZ-16 at ^{1}H field strengths of 6 kHz. Typical rf pulse lengths were ~4 μs for ^{31}P.

3. Results and discussion

Static ^{31}P chemical shift anisotropy NMR measurements were conducted at variable temperatures (280 K–360 K) to determine if any changes in membrane morphology or lipid transition temperatures occurred upon peptide binding. The ^{31}P NMR spectra of the model mitochondrial membranes alone (Fig. 2a) were recorded to provide a comparison to the peptide-bound membranes (Fig. 2b). The observed static ^{31}P NMR lineshape is consistent with hydrated 100 nm unilamellar vesicles, as is the observed linewidth (~2 kHz), even at the highest temperature of 360 K [78]. The alterations in ^{31}P lineshape at each temperature are a reflection of the unique transition temperatures for each of the lipids, ranging from 264 K for PC to 347 K for PE, and the resulting mixed liquid crystalline and gel phases. For the peptide-containing samples, the MPP was added at a peptide to lipid ratio of P:L = 1:12.5. This peptide concentration is sufficiently high to observe membrane defects, if they are present upon binding. No significant remodeling of the lipid bilayer was observed at any temperature, indicating that peptide insertion did not disrupt the lamellarity of the bilayer. This observation is consistent with the non-lytic nature of other penetrating peptides [38,79–81]. Furthermore, no isotropic peak was observed, ruling out the possibility of the formation of inverse micelles to internalize the peptide.

To assess the remaining two mechanisms of translocation (electroporation and guanidinium-phosphate complexation), we used a ^{13}C MAS NMR PRE method at 310 K [24]. In order to assure we could achieve asymmetric distribution of Mn^{2+} paramagnetic ions with our new model inner mitochondrial membranes, we first monitored the ion position with the ^{31}P NMR signal of the lipid headgroups (Fig. 3). Without paramagnetic ions present, we measured the entire signal from all the phospholipid headgroups. The addition of Mn^{2+} to the outside of the vesicles caused signal attenuation of about half the lipids, corresponding to dephasing of the outer leaflet. When the paramagnetic ions are on both sides of the bilayer, the

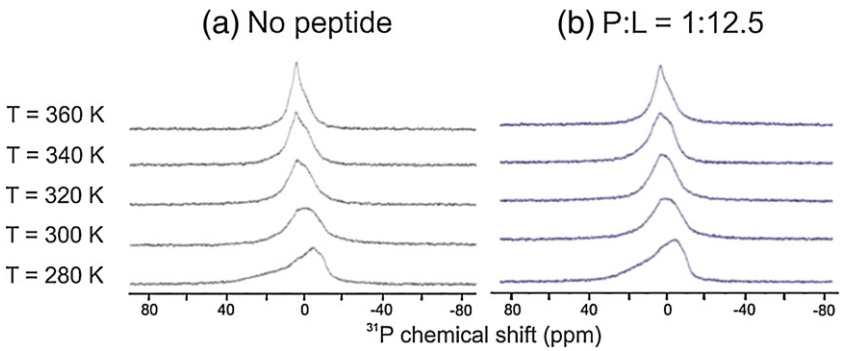

Fig. 2. The peptide does not dramatically alter the structure of the membrane. Static ^{31}P NMR spectra of liposomes (a) in the absence of MPP and (b) in the presence of MPP. Because there is no change in the chemical shift anisotropy of the lipid headgroups, there is no remodeling of the bilayer morphology. The absence of an isotropic peak allows the inverse micelle mechanism to be ruled out.

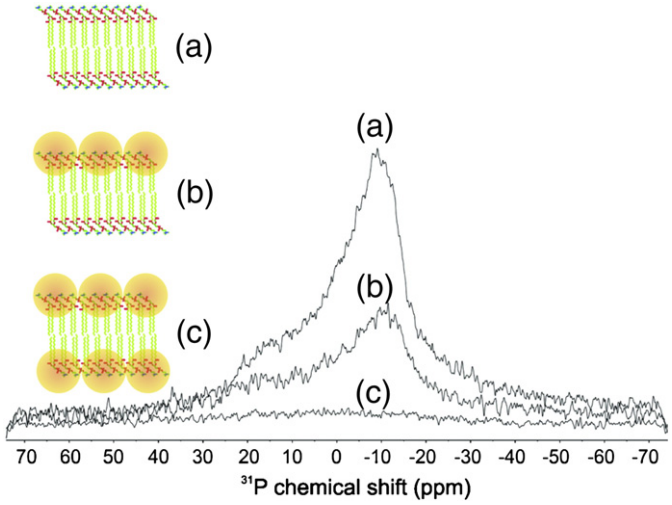

Fig. 3. Mn^{2+} ions do not cross the bilayer and form stable one side bound samples. Static ^{31}P NMR spectra of (a) unbound, (b) one side Mn^{2+} bound with 47% dephasing, and (c) two side Mn^{2+} bound with 100% dephasing CL/PC/PE LUVs.

entire ^{31}P signal is killed because all lipid headgroups are in close proximity to Mn^{2+}. This experiment showed that Mn^{2+} ions bind to lipid headgroups, but do not diffuse through the model inner mitochondrial membranes, even in the presence of a negative transmembrane gradient, allowing asymmetric Mn^{2+} distribution to probe insertion depth and determine bilayer sidedness, consistent with previously reported spectra in the absence of a transmembrane gradient [24]. Since the addition of paramagnetic ions to the system may perturb the electrostatic interactions in subsequent membrane–peptide experiments, we added the minimal amount of Mn^{2+} to achieve suitable signal attenuation, at 8 mol% of the lipid concentration. The peptide affinity for the membrane should not be affected by this minimal anionic phosphate charge neutralization of 8 mol%.

In order to determine whether peptide insertion is concentration dependent, the MPP was added to the membranes at two different peptide concentrations. Fig. 4 shows the ^{13}C DP-MAS NMR results of the PRE effect of one and two side Mn^{2+} bound membranes at both peptide concentrations. The lipid peaks are attenuated as expected in all samples. In the one side Mn^{2+} bound sample at P:L = 1:10, the peptide peaks retain much of the signal intensity (~75%) when compared to the unbound sample. However, in the two side Mn^{2+} bound spectra, much of the peptide peak intensity is dephased, with signal retention dropping to about 50%, on average. This is consistent with the MPP partitioning into both leaflets of the bilayer at high concentration.

Fig. 5 shows a graphical representation of the PRE effect on the normalized signal intensity for both low (P:L = 1:40) and high (P:L = 1:10) peptide concentrations. In order to compare between different samples, the NMR signal peak intensity was double-normalized, $(S / S_0) / (S / S_0)_{max}$, where S is the signal of the Mn^{2+} bound sample, S_0 is the Mn^{2+} free sample, and $(S / S_0)_{max}$ is the normalized value of the lipid peak with the least attenuation. The error bars were obtained via error propagation of the signal to noise ratio of each peak. At low P:L = 1:40, there is no change in signal intensity when comparing one side and two side Mn^{2+} bound membranes (Fig. 4), placing the peptide solely in the outer leaflet. At high P:L = 1:10, the peptide retains much of its signal intensity in the one side Mn^{2+} bound sample, while in the two side Mn^{2+} bound sample, the signal intensity is significantly lowered. Therefore, we can conclude that at low peptide concentrations, the MPP binds only to the outer leaflet while at high peptide concentrations the MPP is distributed in both the inner and outer leaflets of the bilayer.

Due to the low signal to noise ratio, and subsequent large error bars for the P:L = 1:40 sample, we wanted to confirm that the peptide was only bound to the outer leaflet of the bilayer. To achieve higher resolution spectra to support this claim, we constructed vesicles with Mn^{2+} bound only to the inside of the vesicles with a P:L = 1:40 and compared the normalized signal intensities to P:L = 1:40 with no Mn^{2+}, and P:L = 1:40 with Mn^{2+} bound only to the outside of the vesicles (Fig. 6). If the peptide was bound to the outer leaflet of the vesicle, Mn^{2+} ions on the inner leaflet only should have no effect of the peptide signal intensities, and that is what we observe. Fig. 6 shows that the peptide signal intensity is retained for the Mn^{2+} inside sample. As expected, the lipid Cγ peak intensity is the same for both the inside Mn^{2+} bound and outside Mn^{2+} bound samples. We also constructed the same vesicles to examine the P:L = 1:10 sample. Nearly the same signal dephasing is observed for both one-sided Mn^{2+} bound samples (inside and outside), confirming that the peptide is distributed into both the inner and outer leaflets, at approximately a 50/50 ratio.

We also used the ^{13}C MAS PRE data as a spectroscopic ruler to estimate the MPP location in the bilayer. Since the depth associated with the lipid peaks is known from the bilayer structure of the vesicles, the signal dephasing of the peptide can be compared to that of the lipids to estimate insertion depth. Fig. 7 shows that at P:L = 1:40, the MPP is inserted at approximately C1–C2, at the top of the acyl chain, in the interfacial region. Due to the larger error associated

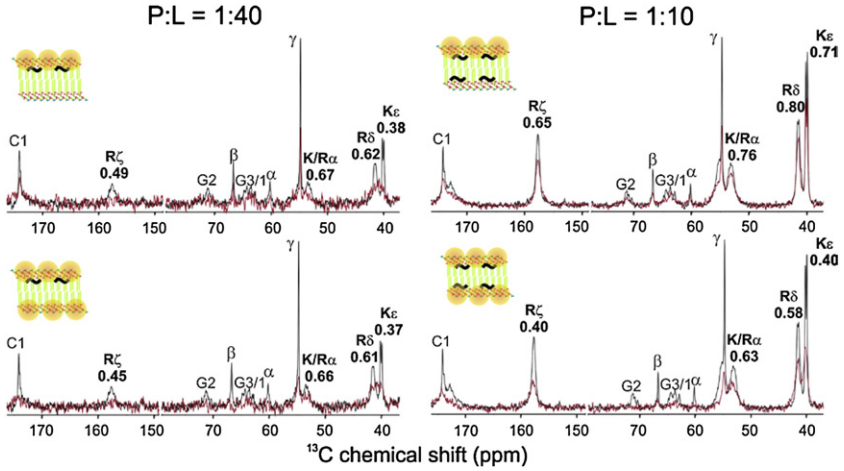

Fig. 4. ^{13}C MAS NMR spectra illustrating the attenuation due to the PRE effect at low (P:L = 1:40) and high (P:L = 1:10) peptide concentration. The membrane schematics indicate the peptide location and PRE effect felt by the peptide:lipid system in one side Mn^{2+} bound (top) and two side Mn^{2+} bound samples. All attenuated spectra (red) are overlaid with the unbound spectra (black) with the fraction of dephasing displayed for the peptide peaks.

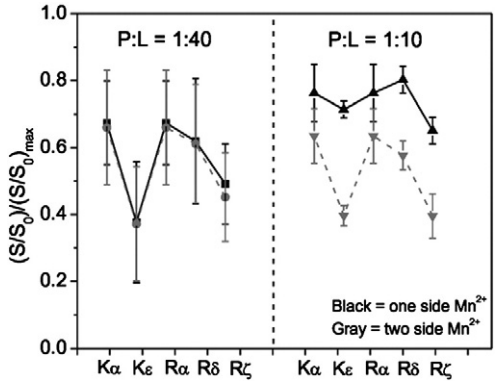

Fig. 5. High peptide concentration leads to distribution in both leaflets. At low P:L = 1:40 the MPP only binds to the outer leaflet because there is no change in the signal intensity. At high P:L = 1:10 the one side Mn^{2+} bound sample shows high signal intensity and the two side Mn^{2+} bound sample shows low signal intensity, indicative of distribution in both leaflets.

with the low concentration peptide sample, we recognize that peptide may be closer to the surface of the bilayer than the high concentration sample, and the signal dephasing serves only as an approximation for insertion depth. Even slight differences in insertion depth can result in larger signal dephasing since the spin–spin relaxation rate in the presence of paramagnetic ions is proportional to r^{-6}, where r is the distance between the paramagnetic center and the observed resonance.

When the ratio is increased to P:L = 1:10, the peptide is distributed into both leaflets. Assuming that half of the peptide is bound to the outer leaflet, and half is bound to the inner leaflet, Fig. 7b–c shows that the MPP is inserted into both leaflets at C2. The peptide interaction at the top of the acyl chain, near C1 (P:L = 1:40) and C2 (P:L = 1:10), indicates stability at this position on the lipid acyl chain, likely due to the close proximity of the cationic peptide to the phospholipid headgroup.

In order to estimate the insertion depth, it was assumed that the peptides are membrane-bound, and not exchanging with the solvent. In the rapid exchange regime, it is possible to estimate the mole fraction of peptide bound by varying the peptide to lipid ratio, and measuring the change in ^{13}C chemical shift as the peptide concentration increases [82]. No change in ^{13}C chemical shift was observed between P:L = 1:40 and P:L = 1:10 for the peptide resonances, indicating that at both concentrations, the peptide is membrane-bound. This observation is consistent with previous studies on short peptides reconstituted in model lipid systems that found that over 90% of the peptides were membrane bound [83,84].

From this information, we found that the concentration-dependent peptide distribution in the inner and outer leaflets of the bilayer supports the electroporation model of translocation. Once bound to the inner leaflet of the bilayer, the peptides can proceed to enter the matrix. The electroporation model provides an explanation as to how and why MPPs translocate through the dense, hydrophobic portion of the inner mitochondrial membrane. The threshold for a sufficient voltage to form pores of electroporation ranges from −250 to −550 mV [44]. In our model membranes, we created a transmembrane gradient of −180 mV that is equivalent to mitochondrial gradients encountered in biological systems. While this gradient alone is not enough to form transient pores, the accumulation of cationic peptides in the outer leaflet can induce an additional potential.

In the case of MPPs interacting with our model membranes, the electrostatic potential of a few peptides binding to the outer leaflet is not strong enough for electroporation because the charge is reduced by counterions on the phosphate headgroups [44]. In particular, PC and PE are both zwitterionic lipids, whereas CL is anionic, with two negatively charged phosphate headgroups. In this case,

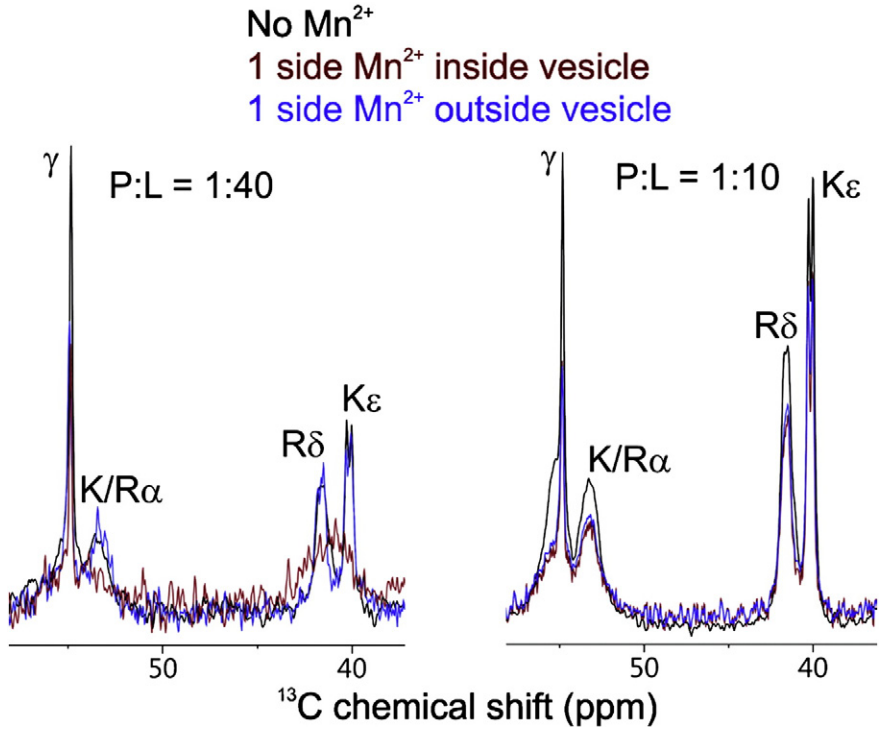

Fig. 6. At P:L = 1:40, the peptide is only bound to the outer leaflet of the vesicle, as determined by ^{13}C MAS PRE NMR. The blue spectra show that within the signal-to noise error, the peptide peaks retain their signal intensity with Mn^{2+} bound only to the inside of the vesicle, demonstrating that the paramagnetic ions have no effect on the peptide that is bound to the outer leaflet. P:L = 1:40 in the absence of Mn^{2+} (black) and Mn^{2+} bound to the outside of the vesicle (red) are shown for comparison. The same experiment was performed for P:L = 1:10. The same signal dephasing is observed whether the one-side Mn^{2+} ions are inside or outside of the vesicles, confirming that the peptide is distributed evenly in both leaflets.

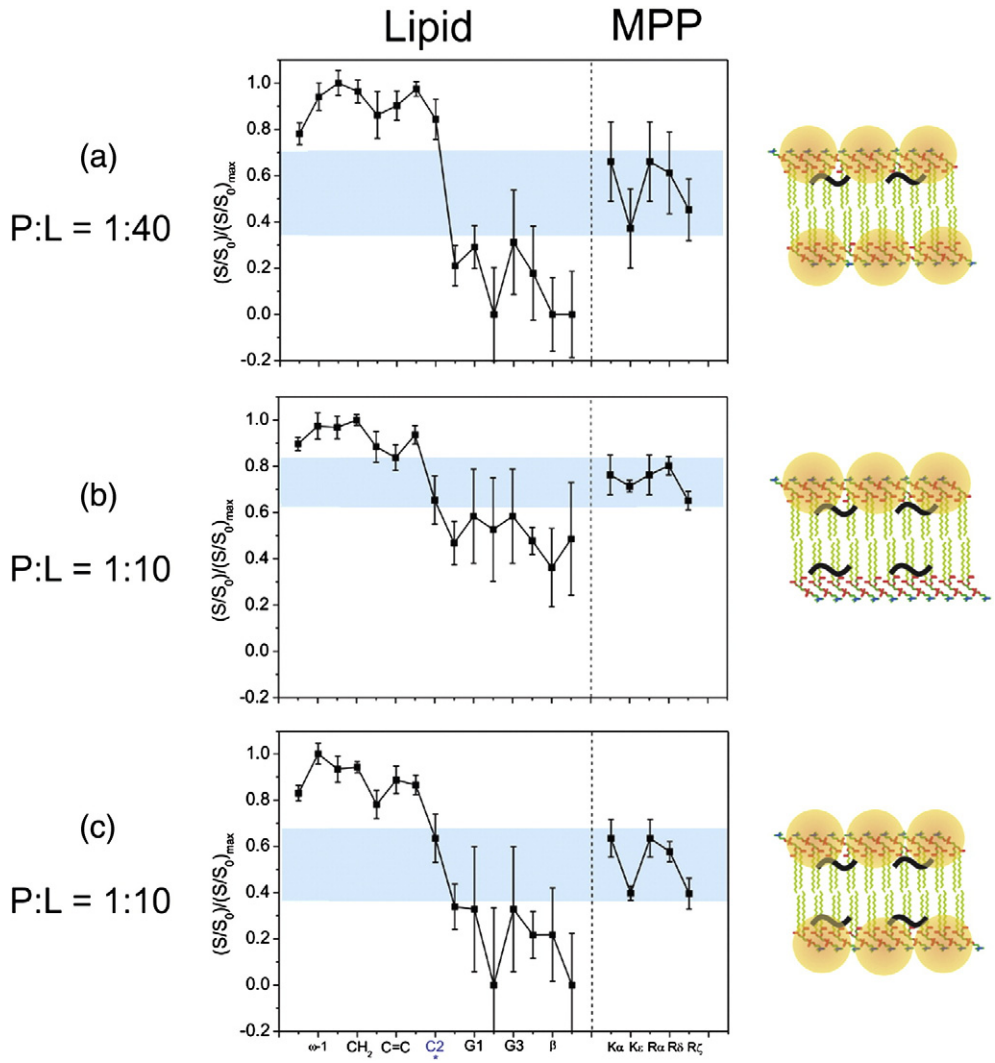

Fig. 7. At both high and low peptide concentrations, the MPP is bound near C2 of the lipid acyl chain. The intensity of the Mn^{2+} bound sample (S) double normalized with respect to the unbound sample (S_0) and the maximum lipid peak $(S / S_0)_{max}$. The shaded region shows the depth of MPP insertion in the bilayer for (a) two side Mn^{2+} with P:L = 1:40, (b) one side Mn^{2+} with P:L = 1:10, and (c) two side Mn^{2+} with P:L = 1: 10.

the two positive charges from the Arg and Lys residues on the MPP are present at a 1:1 ratio with the negative charges on the cardiolipin headgroup. Given that the concentration of CL in our model membranes is 10%, to reflect the occurrence in mammalian mitochondria, peptide-to-lipid ratio of 1:40 would not fully neutralize the anionic charge in the outer leaflet, assuming an even distribution of anionic charge in both monolayers. Once an adequate amount of MPPs, the threshold concentration, also bind, the peptides provide enough surface charge density to attract additional anionic lipids in the inner leaflet to provide sufficient voltage to permit passage through the formation of transient pores [44]. At a concentration of 1:10, the anionic character of the outer leaflet is fully saturated with cationic peptides, leading to an electroporation-like transfer of peptides to the inner leaflet, as revealed in the ^{13}C PRE NMR spectra. The concentration dependence of translocation observed here is consistent with the electroporation model for internalization. The MPP is able to cross the high energy barrier of the hydrophobic bilayer core, in spite of membrane curvature, which can play a role in preventing penetrating-peptide translocation [85], and is likely stabilized by cardiolipin [86,87].

The influence of electrostatic interaction between anionic phospholipids and cationic cell-penetrating peptides has been well-studied. While hydrophobic interactions between the bilayer core and hydrophobic peptide residues were found to contribute to peptide translocation [88], several studies have found that the electrostatic attraction between negatively charged lipids and positively charged residues dominates the initial binding event [23,25,88–95]. There is substantial evidence that the anionic phospholipid electrostatic contribution can be a minor compared to the total lipid population and still have an effect on penetrating-peptide binding and structural reorganization [89,91,92]. Furthermore, the anionic phospholipid–cationic peptide interaction is stronger for Arg residues than Lys residues, indicating the necessity of Arg residues to facilitate membrane insertion, especially into the plasma membrane [94].

For MPPs, the presence of Arg clusters has been shown to increase transport across the plasma membrane, but resulted in a decrease in mitochondrial localization [10]. Therefore, the requirement for mitochondrial membrane penetration is likely different than that of the plasma membrane, which is probably a delicate balance between electrostatic and hydrophobic interactions between the bilayer, peptides, and electrochemical gradient.

Similar NMR measurements were performed previously on a well known cell-penetrating peptide, penetratin [24]. The translocation of penetratin was examined in lipid vesicles without a transmembrane gradient and that contained ~50% anionic character. Penetratin has seven cationic residues, and at both high (P:L = 1:10) and low (P:L = 1:40) concentrations, it was shown to be distributed into both leaflets of the

bilayer, even though the negatively charged phospholipid headgroups never become fully neutralized. This mechanism of internalization was attributed to a guanidinium-phosphate complexation that allowed the peptide to cross the hydrophobic portion of the bilayer without a high free-energy penalty, differing from the previously proposed models [24]. The inner mitochondrial membranes presented here should allow easier translocation, due to the presence of a transmembrane gradient, as well as a lower anionic content, that would become saturated more quickly. Yet, we observe a concentration dependent mode of translocation, consistent with the electroporation model. This evidence suggests that different classes of penetrating peptides proceed with internalization via different mechanisms which may be lipid membrane and transmembrane gradient dependent.

Previous studies have implicated the importance of a transmembrane gradient to penetrating-peptide internalization [96–98], and since transmembrane potential was shown to be equally important for MPPs [10], we were motivated to create model membranes that exhibited a electrochemical gradient. To examine the influence of a transmembrane gradient on our system, we considered the energy barriers the MPP had to overcome in order to go from the outer leaflet, through the hydrophobic center of the bilayer, to the inner leaflet of the bilayer (Fig. 8). The energy cost of each step was estimated using the Wimley–White interfacial hydrophobicity scale determined from measurements of short peptides partitioning into zwitterionic phosphatidylcholine (POPC) vesicles and *n*-octanol [99–101]. For our system, we estimated a favorable, negative free energy change for insertion into the interfacial region. The MPP then has to overcome an unfavorable, positive energy barrier to cross the bilayer core. Then, the peptide can fall back into the favorable interfacial region of the inner leaflet.

If we examine the force across the plasma membrane, F = 12 kJ/mol (assuming the membrane potential is −60 mV), this is sufficient to pull the cationic peptide across the free energy barrier in the hydrocarbon core and overcome the stabilizing forces present in the interfacial region to enter the cytosol. The OMM contains pore-like structures called porins, which allow the passage of small peptides [11]. Here, the peptide can electrostatically interact with the anionic IMM. Because the IMM is anionic, rather than zwitterionic, the favorable free energy associated with the water–membrane interface will be lower than the calculated values (dotted red lines in Fig. 8). The IMM exhibits a transmembrane potential of −180 mV, providing a force of 36 kJ/mol. Assuming the transmembrane gradient is the only force acting on the peptide, if it is enough to pull the peptide over the high free energy barrier of the bilayer core (we see distribution in both leaflets at high peptide concentration), it should be enough to move the peptide from the interfacial region to the matrix, unless the peptide–lipid interaction provides enough stability to lock the MPP in the interfacial region. While it has been indicated that only a small percentage of peptides with similar amino acid sequences, SS tetrapeptides [102], reach the matrix, recent studies on several MPPs are consistent with matrix localization [103], suggesting these peptides undergo full internalization.

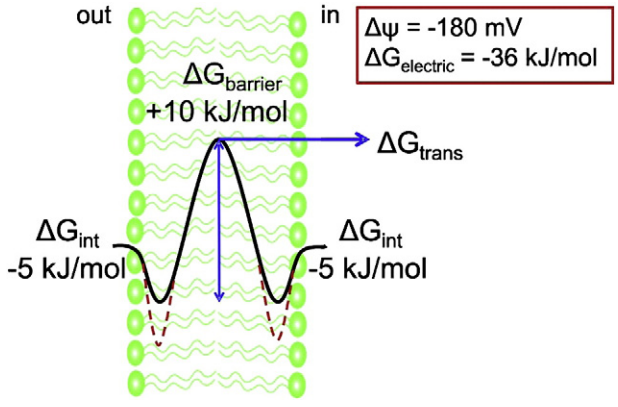

Fig. 8. The energy profile associated with inserting the MPP into a plasma membrane (black) and the inner mitochondrial membrane (red). The MPP is inserted into the interfacial region of the outer leaflet. The MPP crosses a free energy barrier to reach the hydrocarbon core of the bilayer. The MPP inserts into the interfacial region of the inner leaflet, where it can be released. The transmembrane potentials provide a driving force for translocation.

4. Conclusions

We successfully constructed model inner mitochondrial membranes, exhibiting a transmembrane gradient of −180 mV that were suitable to study peptide–lipid interactions with ssNMR. The inner mitochondrial membranes were used to gain insight into the mechanism of translocation of a mitochondria-penetrating peptide. By using variable temperature static ^{31}P NMR spectroscopy, we were able to determine that the peptide did not disrupt the lamellarity of the bilayer, nor did it affect the phase transition temperatures. We established that the membranes were also conducive to perform asymmetric insertion depth measurements, due to their non-permeable nature with respect to Mn^{2+} ions, using ^{13}C MAS PRE experiments. At low peptide concentrations, the MPP binds only to the outer leaflet of the bilayer, at C2 near the top of the lipid acyl chain. As the concentration is increased, the peptide passes through the hydrophobic core of the membrane and redistributes into both leaflets of the bilayer. These measurements provide evidence that the MPP in this paper follows the electroporation model for translocation.

Acknowledgements

This work was funded by NSF Career Award 0847417.

References

[1] C.A. Bradham, T. Qian, K. Streetz, C. Trautwein, D.A. Brenner, J.J. Lemasters, The mitochondrial permeability transition is required for tumor necrosis factor alpha-mediated apoptosis and cytochrome c release, Mol. Cell. Biol. 18 (1998) 6353–6364.
[2] M. Corral-Debrinski, J.M. Shoffner, M.T. Lott, D.C. Wallace, Association of mitochondrial DNA damage with aging and coronary atherosclerotic heart disease, Mutation Research/DNAging 275 (1992) 169–180.
[3] R. Ferrari, The role of mitochondria in ischemic heart disease, J. Cardiovasc. Pharmacol. 28 (1996) 1–10.
[4] V. Goossens, J. Grooten, K. De Vos, W. Fiers, Direct evidence for tumor necrosis factor-induced mitochondrial reactive oxygen intermediates and their involvement in cytotoxicity, Proc. Natl. Acad. Sci. U.S.A. 92 (1995) 8115–8119.
[5] R.P. Hafner, M.J. Leake, M.D. Brand, Hypothyroidism in rats decreases mitochondrial inner membrane cation permeability, FEBS Lett. 248 (1989) 175–178.
[6] A.T. Hoye, J.E. Davoren, P. Wipf, M.P. Fink, V.E. Kagan, Targeting mitochondria, Accounts of Chemical Research 41 (2008) 87–97.
[7] E.J. Lesnefsky, S. Moghaddas, B. Tandler, J. Kerner, C.L. Hoppel, Mitochondrial dysfunction in cardiac disease: ischemia–reperfusion, aging, and heart failure, J. Mol. Cell. Cardiol. 33 (2001) 1065–1089.
[8] G. Paradies, G. Petrosillo, F.M. Ruggiero, Cardiolipin-dependent decrease of cytochrome c oxidase activity in heart mitochondria from hypothyroid rats, Biochimica et Biophysica Acta (BBA) — Bioenergetics 1319 (1997) 5–8.
[9] S.G. Pavlakis, P.C. Phillips, S. DiMauro, D.C. De Vivo, L.P. Rowland, Mitochondrial myopathy, encephalopathy, lactic acidosis, and strokelike episodes: a distinctive clinical syndrome, Ann. Neurol. 16 (1984) 481–488.
[10] K.L. Horton, K.M. Stewart, S.B. Fonseca, Q. Guo, S.O. Kelley, Mitochondria-penetrating peptides, Chem. Biol. 15 (2008) 375–382.
[11] I.E. Scheffler, Mitochondria, John Wiley & Sons, Inc., Hoboken, New Jersey, 2008.
[12] L.F. Yousif, K.M. Stewart, K.L. Horton, S.O. Kelley, Mitochondria-penetrating peptides: sequence effects and model cargo transport, Chembiochem 10 (2009) 2081–2088.
[13] L.F. Yousif, K.M. Stewart, S.O. Kelley, Targeting mitochondria with organelle-specific compounds: strategies and applications, Chembiochem 10 (2009) 1939–1950.
[14] M.P. Pereira, S.O. Kelley, Maximizing the therapeutic window of an antimicrobial drug by imparting mitochondrial sequestration in human cells, J. Am. Chem. Soc. 133 (2011) 3260–3263.
[15] L.B. Andreas, M.T. Eddy, R.M. Pielak, J. Chou, R.G. Griffin, Magic angle spinning NMR investigation of influenza A M218–60: support for an allosteric mechanism of inhibition, J. Am. Chem. Soc. 132 (2010) 10958–10960.
[16] B. Bechinger, E.S. Salnikov, The membrane interactions of antimicrobial peptides revealed by solid-state NMR spectroscopy, Chem. Phys. Lipids 165 (2012) 282–301.
[17] M. Hong, Oligomeric structure, dynamics, and orientation of membrane proteins from solid-state NMR, Structure 14 (2006) 1731–1740.

[18] M. Hong, Y. Su, Structure and dynamics of cationic membrane peptides and proteins: insights from solid-state NMR, Protein Sci. 20 (2011) 641–655.
[19] M. Hong, Y. Zhang, F. Hu, Membrane protein structure and dynamics from NMR spectroscopy, Annu. Rev. Phys. Chem. 63 (2012) 1–24.
[20] E.F. Palermo, D.-K. Lee, A. Ramamoorthy, K. Kuroda, Role of cationic group structure in membrane binding and disruption by amphiphilic copolymers, J. Phys. Chem. B 115 (2010) 366–375.
[21] A. Ramamoorthy, Beyond NMR spectra of antimicrobial peptides: dynamical images at atomic resolution and functional insights, Solid State Nucl. Magn. Reson. 35 (2009) 201–207.
[22] E.S. Salnikov, A.J. Mason, B. Bechinger, Membrane order perturbation in the presence of antimicrobial peptides by ^{2}H solid-state NMR spectroscopy, Biochimie 91 (2009) 734–743.
[23] Y. Su, T. Doherty, A.J. Waring, P. Ruchala, M. Hong, Roles of arginine and lysine residues in the translocation of a cell-penetrating peptide from ^{13}C, ^{31}P, and ^{19}F solid-state NMR, Biochemistry 48 (2009) 4587–4595.
[24] Y. Su, R. Mani, M. Hong, Asymmetric insertion of membrane proteins in lipid bilayers by solid-state NMR paramagnetic relaxation enhancement: a cell-penetrating peptide example, J. Am. Chem. Soc. 130 (2008) 8856–8864.
[25] Y. Su, A.J. Waring, P. Ruchala, M. Hong, Membrane-bound dynamic structure of an arginine-rich cell-penetrating peptide, the protein transduction domain of HIV TAT, from solid-state NMR, Biochemistry 49 (2010) 6009–6020.
[26] T. Doherty, Y. Su, M. Hong, High-resolution orientation and depth of insertion of the voltage-sensing S4 helix of a potassium channel in lipid bilayers, J. Mol. Biol. 401 (2010) 642–652.
[27] S. Unnerståle, F. Madani, A. Gräslund, L. Mäler, Membrane-perturbing properties of two Arg-rich paddle domains from voltage-gated sensors in the KvAP and HsapBK K^{+} channels, Biochemistry 51 (2012) 3982–3992.
[28] Y. Su, F. Hu, M. Hong, Paramagnetic Cu(II) for probing membrane protein structure and function: inhibition mechanism of the influenza M2 proton channel, J. Am. Chem. Soc. 134 (2012) 8693–8702.
[29] E. Teissier, G. Zandomeneghi, A. Loquet, D. Lavillette, J.-P. Lavergne, R. Montserret, F.-L. Cosset, A. Böckmann, B.H. Meier, F. Penin, E.-I. Pécheur, Mechanism of inhibition of enveloped virus membrane fusion by the antiviral drug arbidol, PLoS One 6 (2011) e15874.
[30] S.J. Opella, S.H. Park, S. Lee, D. Jones, A. Nevzorov, M. Mesleh, A. Mrse, F.M. Marassi, M. Oblatt-Montal, M. Montal, K. Strebel, S. Bour, Structure and function of Vpu from HIV-1, in: W. Fischer (Ed.), Viral Membrane Proteins: Structure, Function, and Drug Design, 1, Springer, US, 2005, pp. 147–163.
[31] R.F. Epand, L. Maloy, A. Ramamoorthy, R.M. Epand, Amphipathic helical cationic antimicrobial peptides promote rapid formation of crystalline states in the presence of phosphatidylglycerol: lipid clustering in anionic membranes, Biophys. J. 98 (2010) 2564–2573.
[32] E.F. Haney, S. Nathoo, H.J. Vogel, E.J. Prenner, Induction of non-lamellar lipid phases by antimicrobial peptides: a potential link to mode of action, Chem. Phys. Lipids 163 (2010) 82–93.
[33] A. Lamazière, C. Wolf, O. Lambert, G. Chassaing, G. Trugnan, J. Ayala-Sanmartin, The homeodomain derived peptide penetratin induces curvature of fluid membrane domains, PLoS One 3 (2008) e1938.
[34] M.F.M. Sciacca, J.R. Brender, D.-K. Lee, A. Ramamoorthy, Phosphatidylethanolamine enhances amyloid fiber-dependent membrane fragmentation, Biochemistry 51 (2012) 7676–7684.
[35] J.B. Rothbard, T.C. Jessop, R.S. Lewis, B.A. Murray, P.A. Wender, Role of membrane potential and hydrogen bonding in the mechanism of translocation of guanidinium-rich peptides into cells, J. Am. Chem. Soc. 126 (2004) 9506–9507.
[36] J.T.J. Cheng, J.D. Hale, M. Elliot, R.E.W. Hancock, S.K. Straus, Effect of membrane composition on antimicrobial peptides aurein 2.2 and 2.3 from australian southern bell frogs, Biophys. J. 96 (2009) 552–565.
[37] Y. Shai, Mechanism of the binding, insertion and destabilization of phospholipid bilayer membranes by α-helical antimicrobial and cell non-selective membrane-lytic peptides, Biochimica et Biophysica Acta (BBA) - Biomembranes 1462 (1999) 55–70.
[38] U. Langel, The Handbook of Cell-Penetrating Peptides, CRC Press Taylor & Francis Group, Boca Raton, FL, 2006.
[39] M. Lindgren, M. Hällbrink, A. Prochiantz, Ü. Langel, Cell-penetrating peptides, Trends Pharmacol. Sci. 21 (2000) 99–103.
[40] J.P. Richard, K. Melikov, E. Vives, C. Ramos, B. Verbeure, M.J. Gait, L.V. Chernomordik, B. Lebleu, Cell-penetrating peptides — a reevaluation of the mechanism of cellular uptake, J. Biol. Chem. 278 (2003) 585–590.
[41] D. Derossi, G. Chassaing, A. Prochiantz, Trojan peptides: the penetratin system for intracellular delivery, Trends Cell Biol. 8 (1998) 84–87.
[42] A. Prochiantz, Getting hydrophilic compounds into cells: lessons from homeopeptides, Curr. Opin. Neurobiol. 6 (1996) 629–634.
[43] H. Binder, G. Lindblom, Charge-dependent translocation of the Trojan peptide penetratin across lipid membranes, Biophys. J. 85 (2003) 982–995.
[44] K. Cahill, Cell-penetrating peptides, electroporation and drug delivery, IET Syst. Biol. 4 (2010) 367–378.
[45] L. Mäler, A. Gräslund, NMR studies of three-dimensional structure and positioning of CPPs in membrane model systems, in, vol. 683, pp. 57-67.
[46] M. Tang, A.J. Waring, M. Hong, Phosphate-mediated arginine insertion into lipid membranes and pore formation by a cationic membrane peptide from solid-state NMR, J. Am. Chem. Soc. 129 (2007) 11438–11446.
[47] J.-X. Lu, K. Damodaran, J. Blazyk, G.A. Lorigan, Solid-state nuclear magnetic resonance relaxation studies of the interaction mechanism of antimicrobial peptides with phospholipid bilayer membranes, Biochemistry 44 (2005) 10208–10217.
[48] J.D. Gehman, F. Luc, K. Hall, T.-H. Lee, M.P. Boland, T.L. Pukala, J.H. Bowie, M.-I. Aguilar, F. Separovic, Effect of antimicrobial peptides from australian tree frogs on anionic phospholipid membranes, Biochemistry 47 (2008) 8557–8565.
[49] L.T. Nguyen, E.F. Haney, H.J. Vogel, The expanding scope of antimicrobial peptide structures and their modes of action, Trends Biotechnol. 29 (2011) 464–472.
[50] Z. Liu, H.J. Vogel, Structural basis for the regulation of L-type voltage-gated calcium channels: interactions between the N-terminal cytoplasmic domain and Ca^{2+}–calmodulin, Front. Mol. Neurosci. 5 (2012).
[51] J.P. Berlose, O. Convert, D. Derossi, A. Brunissen, G. Chassaing, Conformational and associative behaviours of the third helix of antennapedia homeodomain in membrane-mimetic environments, Eur. J. Biochem. 242 (1996) 372–386.
[52] J.J. Chou, J.D. Kaufman, S.J. Stahl, P.T. Wingfield, A. Bax, Micelle-induced curvature in a water-insoluble HIV-1 Env peptide revealed by NMR dipolar coupling measurement in stretched polyacrylamide gel, J. Am. Chem. Soc. 124 (2002) 2450–2451.
[53] E.J. Dufourc, I.C.P. Smith, J. Dufourcq, Molecular details of melittin-induced lysis of phospholipid membranes as revealed by deuterium and phosphorus NMR, Biochemistry 25 (1986) 6448–6455.
[54] M. Ouellet, N. Voyer, M. Auger, Membrane interactions and dynamics of a 21-mer cytotoxic peptide: a solid-state NMR study, Biochim. Biophys. Acta 1798 (2010) 235–243.
[55] Y. Su, M. Hong, Conformational disorder of membrane peptides investigated from solid-state NMR line widths and line shapes, J. Phys. Chem. B 115 (2011) 10758–10767.
[56] X. Yu, S. Chu, A.E. Hagerman, G.A. Lorigan, Probing the interaction of polyphenols with lipid bilayers by solid-state NMR spectroscopy, J. Agr. Food Chem. 59 (2011) 6783–6789.
[57] G.P. Holland, S.K. McIntyre, T.M. Alam, Distinguishing individual lipid headgroup mobility and phase transitions in raft-forming lipid mixtures with ^{31}P MAS NMR, Biophys. J. 90 (2006) 4248–4260.
[58] S. Abu-Baker, G.A. Lorigan, Phospholamban and its phosphorylated form interact differently with lipid bilayers: a ^{31}P, ^{2}H, and ^{13}C solid-state NMR spectroscopic study, Biochemistry 45 (2006) 13312–13322.
[59] S. Abu-Baker, X. Qi, G.A. Lorigan, Investigating the interaction of saposin s with POPS and POPC phospholipids: a solid-state NMR spectroscopic study, Biophys. J. 93 (2007) 3480–3490.
[60] N. Bloembergen, Proton relaxation times in paramagnetic solutions, J. Chem. Phys. 27 (1957) 572–573.
[61] I. Solomon, Relaxation processes in a system of two spins, Phys. Rev. 99 (1955) 559.
[62] V.V. Kumar, W.J. Baumann, Lanthanide-induced phosphorus-31 NMR downfield chemical shifts of lysophosphatidylcholines are sensitive to lysophospholipid critical micelle concentration, Biophys. J. 59 (1991) 103–107.
[63] V.V. Kumar, B. Malewicz, W.J. Baumann, Lysophosphatidylcholine stabilizes small unilamellar phosphatidylcholine vesicles. Phosphorus-31 NMR evidence for the "wedge" effect, Biophys. J. 55 (1989) 789–792.
[64] C.P. Jaroniec, Solid-state nuclear magnetic resonance structural studies of proteins using paramagnetic probes, Solid State Nucl. Mag. 43–44 (2012) 1–13.
[65] P. Nadaud, I. Sengupta, J. Helmus, C. Jaroniec, Evaluation of the influence of intermolecular electron-nucleus couplings and intrinsic metal binding sites on the measurement of ^{15}N longitudinal paramagnetic relaxation enhancements in proteins by solid-state NMR, J. Biomol. NMR 51 (2011) 293–302.
[66] P.S. Nadaud, J.J. Helmus, S.L. Kall, C.P. Jaroniec, Paramagnetic ions enable tuning of nuclear relaxation rates and provide long-range structural restraints in solid-state NMR of proteins, J. Am. Chem. Soc. 131 (2009) 8108–8120.
[67] P.S. Nadaud, J.J. Helmus, I. Sengupta, C.P. Jaroniec, Rapid acquisition of multidimensional solid-state NMR spectra of proteins facilitated by covalently bound paramagnetic tags, J. Am. Chem. Soc. 132 (2010) 9561–9563.
[68] I. Sengupta, P.S. Nadaud, J.J. Helmus, C.D. Schwieters, C.P. Jaroniec, Protein fold determined by paramagnetic magic-angle spinning solid-state NMR spectroscopy, Nat. Chem. 4 (2012) 410–417.
[69] S. Parthasarathy, F. Long, Y. Miller, Y. Xiao, D. McElheny, K. Thurber, B. Ma, R. Nussinov, Y. Ishii, Molecular-level examination of Cu^{2+} binding structure for amyloid fibrils of 40-residue Alzheimer's β by solid-state NMR spectroscopy, J. Am. Chem. Soc. 133 (2011) 3390–3400.
[70] K. Yamamoto, J. Xu, K.E. Kawulka, J.C. Vederas, A. Ramamoorthy, Use of a copper-chelated lipid speeds up NMR measurements from membrane proteins, J. Am. Chem. Soc. 132 (2010) 6929–6931.
[71] J. Iwahara, D.E. Anderson, E.C. Murphy, G.M. Clore, EDTA-derivatized deoxythymidine as a tool for rapid determination of protein binding polarity to DNA by intermolecular paramagnetic relaxation enhancement, J. Am. Chem. Soc. 125 (2003) 6634–6635.
[72] J. Iwahara, G.M. Clore, Detecting transient intermediates in macromolecular binding by paramagnetic NMR, Nature 440 (2006) 1227–1230.
[73] S.H. Park, C. Loudet, F.M. Marassi, E.J. Dufourc, S.J. Opella, Solid-state NMR spectroscopy of a membrane protein in biphenyl phospholipid bicelles with the bilayer normal parallel to the magnetic field, J. Magn. Reson. 193 (2008) 133–138.
[74] S. Chu, S. Maltsev, A.H. Emwas, G.A. Lorigan, Solid-state NMR paramagnetic relaxation enhancement immersion depth studies in phospholipid bilayers, J. Magn. Reson. 207 (2010) 89–94.
[75] P.R. Cullis, M.B. Bally, T.D. Madden, L.D. Mayer, M.J. Hope, pH gradients and membrane transport in liposomal systems, Trends Biotechnol. 9 (1991) 268–272.
[76] D. Terrone, S.L.W. Sang, L. Roudaia, J.R. Silvius, Penetratin and related cell-penetrating cationic peptides can translocate across lipid bilayers in the presence of a transbilayer potential, Biochemistry 42 (2003) 13787–13799.
[77] D.W. Deamer, R.C. Prince, A.R. Crofts, The response of fluorescent amines to pH gradients across liposome membranes, Biochim. Biophys. Acta 274 (1972) 323–335.

[78] M. Traikia, D.E. Warschawski, M. Recouvreur, J. Cartaud, P.F. Devaux, Formation of unilamellar vesicles by repetitive freeze-thaw cycles: characterization by electron microscopy and P-31-nuclear magnetic resonance, Eur. Biophys. J. Biophys. Lett. 29 (2000) 184–195.
[79] S. Deshayes, M.C. Morris, G. Divita, F. Heitz, Cell-penetrating peptides: tools for intracellular delivery of therapeutics, Cell. Mol. Life Sci. 62 (2005) 1839–1849.
[80] M. Hansen, K. Kilk, Ü. Langel, Predicting cell-penetrating peptides, Adv. Drug Deliv. Rev. 60 (2008) 572–579.
[81] M. Zorko, Ü. Langel, Cell-penetrating peptides: mechanism and kinetics of cargo delivery, Adv. Drug Deliv. Rev. 57 (2005) 529–545.
[82] C.M. Deber, B.A. Behnam, Role of membrane lipids in peptide hormone function: binding of enkephalins to micelles, Proc. Natl. Acad. Sci. 81 (1984) 61–65.
[83] C.R. Sanders, G.C. Landis, Facile acquisition and assignment of oriented sample NMR spectra for bilayer surface-associated proteins, J. Am. Chem. Soc. 116 (1994) 6470–6471.
[84] C.R. Sanders, G.C. Landis, Reconstitution of membrane proteins into lipid-rich bilayered mixed micelles for NMR studies, Biochemistry 34 (1995) 4030–4040.
[85] D. Persson, P.E.G. Thorén, E.K. Esbjörner, M. Goksör, P. Lincoln, B. Nordén, Vesicle size-dependent translocation of penetratin analogs across lipid membranes, BBA - Biomembranes 1665 (2004) 142–155.
[86] N. Khalifat, N. Puff, S. Bonneau, J.-B. Fournier, M.I. Angelova, Membrane deformation under local pH gradient: mimicking mitochondrial cristae dynamics, Biophys. J. 95 (2008) 4924–4933.
[87] N. Tomsie, B. Babnik, D. Lombardo, B. Mavcic, M. Kandušer, A. Iglic, V. Kralj-Iglic, Shape and size of giant unilamellar phospholipid vesicles containing cardiolipin, J. Chem. Info. Mod. 45 (2005) 1676–1679.
[88] C. Schwieger, A. Blume, Interaction of Poly(L-arginine) with negatively charged dppg membranes: calorimetric and monolayer studies, Biomacromolecules 10 (2009) 2152–2161.
[89] M.E. Herbig, U. Fromm, J. Leuenberger, U. Krauss, A.G. Beck-Sickinger, H.P. Merkle, Bilayer interaction and localization of cell penetrating peptides with model membranes: a comparative study of a human calcitonin (hCT)-derived peptide with pVEC and pAntp(43–58), Biochim. Biophys. Acta-Biomembr. 1712 (2005) 197–211.
[90] S. Kawamoto, M. Takasu, T. Miyakawa, R. Morikawa, T. Oda, S. Futaki, H. Nagao, Binding of Tat peptides on DOPC and DOPG lipid bilayer membrane studied by molecular dynamics simulations, Mol. Simul. 38 (2012) 366–368.
[91] M.F. Lensink, B. Christiaens, J. Vandekerckhove, A. Prochiantz, M. Rosseneu, Penetratin-membrane association: W48/R52/W56 shield the peptide from the aqueous phase, Biophys. J. 88 (2005) 939–952.
[92] M. Magzoub, L.E.G. Eriksson, A. Graslund, Conformational states of the cell-penetrating peptide penetratin when interacting with phospholipid vesicles: effects of surface charge and peptide concentration, Biochim. Biophys. Acta-Biomembr. 1563 (2002) 53–63.
[93] M. Magzoub, K. Kilk, L.E.G. Eriksson, U. Langel, A. Graslund, Interaction and structure induction of cell-penetrating peptides in the presence of phospholipid vesicles, BBA — Biomembranes 1512 (2001) 77–89.
[94] Y. Takechi, H. Tanaka, H. Kitayama, H. Yoshii, M. Tanaka, H. Saito, Comparative study on the interaction of cell-penetrating polycationic polymers with lipid membranes, Chem. Phys. Lipids 165 (2012) 51–58.
[95] A. Ziegler, X.L. Blatter, A. Seelig, J. Seelig, Protein transduction domains of HIV-1 and SIV TAT interact with charged lipid vesicles, Binding Mechanism and Thermodynamic Analysis, Biochemistry 42 (2003) 9185–9194.
[96] J. Bjorklund, H. Biverstahl, A. Graslund, L. Maler, P. Brzezinski, Real-time transmembrane translocation of penetratin driven by light-generated proton pumping, Biophys. J. 91 (2006) L29–L31.
[97] H.D. Herce, A.E. Garcia, J. Litt, R.S. Kane, P. Martin, N. Enrique, A. Rebolledo, V. Milesi, Arginine-rich peptides destabilize the plasma membrane, consistent with a pore formation translocation mechanism of cell-penetrating peptides, Biophys. J. 97 (2009) 1917–1925.
[98] M. Magzoub, A. Pramanik, A. Graslund, Modeling the endosomal escape of cell-penetrating peptides: transmembrane pH gradient driven translocation across phospholipid bilayers, Biochemistry 44 (2005) 14890–14897.
[99] K. Hristova, S.H. White, An experiment-based algorithm for predicting the partitioning of unfolded peptides into phosphatidylcholine bilayer interfaces, Biochemistry 44 (2005) 12614–12619.
[100] W. Wimley, S. White, Experimentally determined hydrophobicity scale for proteins at membrane interfaces, Nat. Struct. Mol. Biol. 3 (1996) 842–848.
[101] W.C. Wimley, T.P. Creamer, S.H. White, Solvation energies of amino acid side chains and backbone in a family of host–guest pentapeptides, Biochemistry 35 (1996) 5109–5124.
[102] K. Zhao, G.-M. Zhao, D. Wu, Y. Soong, A.V. Birk, P.W. Schiller, H.H. Szeto, Cell-permeable peptide antioxidants targeted to inner mitochondrial membrane inhibit mitochondrial swelling, oxidative cell death, and reperfusion injury, J. Biol. Chem. 279 (2004) 34682–34690.
[103] S.B. Fonseca, M.P. Pereira, R. Mourtada, M. Gronda, K.L. Horton, R. Hurren, M.D. Minden, A.D. Schimmer, S.O. Kelley, Rerouting chlorambucil to mitochondria combats drug deactivation and resistance in cancer cells, Chem. Biol. 18 (2011) 445–453.